Detailed Study on the Role of Laser Sintering in Rapid Prototype-Review

***Fathima Hamaza Hasseem Deen, **Saleha Rahman, #Janani Kavi Priya V S**

**UG Student, Department of Chemical Engineering, SEGI University, Malaysia, J.P Lane Puttalam, Srilanka*
***UG Student, Department of Biotechnology, Visvesvaraya Technological University, JHBCS Layout, Bangalore, India*
#Supervisor, Department of Research & Development, Abyom SpaceTech & Defense Pvt. Ltd, Uttar Pradesh, India

Received: 10 January, 2022 Accepted: 22 February, 2022 Online: 05 March, 2022

ABSTRACT

Selective laser sintering, which can employ a wide range of powdered materials to manufacture high quality complex geometries directly from digital models, has become a very adaptable fast prototyping method in recent years. This is one of the powder-based manufacturing methods that employs high-power CO2 laser radiation to melt and fuse polymer powders at a low scanning speed. Surface tension causes balling, therefore high power and moderate scanning speed assist to decrease it. Laser beam design for sintering power material is influenced by technical characteristics such as laser power, temperature, laser point size, scanning speed, and so on. This article offers a detailed evaluation of the effects of different parameters on selective laser sintering incudes Laser power, scanning speed, and temperature. As an outcome, High temperatures promote powder agglomeration, which affects the mechanical integrity, dimensional accuracy, and surface polish of printed components. The melting time will be longer if the scanning speed is low, while the laser energy transfer time will be shorter if the scanning speed is high. When the laser power is too high, and too low cases are discussed along with Mechanical qualities improve as laser power and scanning speed drop, which is consistent with microstructure.

Keywords: *Selective Laser Sintering, scanning speed, laser power, temperature, mechanical properties*

INTRODUCTION

Rapid prototyping refers to a set of methods for quickly fabricating a scale model of a physical part or assembly from 3D computer-aided design (CAD) data. Rapid prototyping is widely used in software engineering to test new business models and application architectures in industries such as automotive, product development, finance, health care, and aerospace. Prototyping is used by aerospace design and industrial teams to develop innovative AM processes in the industry. Rapid prototyping allows designers and developers to get a good sense of how the finished product will look before investing a lot of time and money into it. [21]. Selective laser sintering is one of the important types of rapid prototyping. The quality of an SLS part is determined by a variety of process and material characteristics, including polymer type, grain size, layer thickness, powder spreading speed, scanning speed, laser power, temperature, etc. [15]. It is a powder-based manufacturing technique that uses high-power CO2 laser radiation to melt and fuse polymer powders at a low scanning speed. It uses atomic diffusion to create objects from the powder. For example, plastic, ceramic, and glass are fusing together to produce a 3D solid using heat from a high-power laser. Surface tension causes balling, so high power and moderate scanning speed help to reduce it. During this process, aluminium oxide is often used due to its high hardness, temperature and electrical resistance. [2]. Furthermore, SLS is a highly flexible rapid prototyping process that can create high-quality, complicated geometries directly from digital models using a wide range of powdered materials. The method uses a specific area of powdered materials, layer by layer, to create solid things [7]. In this process, a layer of powder will be deposited onto the platform, and the powder will be flattened. After that, the laser beam enters into the platform and melts the deposited powder, and then the powder surface will be lowered to one layer thickness and finally the 3D object will be constructed. The excess powders will be recycled [14]. This paper will review some important parameters that are used in the SLS process.

LITERATURE REVIEW

Song J.L, et al (2006) The experiment was conducted by 3kW cross flow CO_2 laser machine using silica sand phenol formaldehyde resin (PF resin) with 99% SiO_2, 0.22% Al_2O_3 and micro-content of TiO_2. The melting point was 1750^0C and softening point range was 105^0C-115^0C. It has been observed that the optimized electric current under experimental condition was 1.0A. 12W power, 650mm/min scanning speed, 3mm laser beam diameter, overlapping 0.5mm and power mixture ratio 11:1. Better sintering effects can be obtained with a medium laser power and lower scanning speed [1].

Sercombe. T.B (2011) Used low power CO_2 laser scans across the surface of the powder, melting the resin and bonding the metal powder together to form the layer. Resin bonded aluminium powder was produced by selective laser sintering. The Aluminium powder used was a pre- alloyed Al 6061. Al to AlN was achieved at low temperature and Mg was used as a catalyst for this formation. Elemental Mg was added to the Al_2O_3 powder to preferentially react with the oxygen in atmosphere [3].

Nitish Kumar, et al (2016) Mainly represented the influence of three parameters of laser power, temperature, and part orientation for the dimensional accuracy (1^{st}, 2^{nd}, 3^{rd}) and micro hardness of part made in selective laser sintering (SLS) technique by using Taguchi method with L_9 Orthogonal array. Experimental factors and corresponding levels (Level 1, 2, 3) were identified by Taguchi method. Using the experimental results signal to voice ratio (S/N) was obtained for each level and design robustness was calculated using S/N ratio. [4].

Muita. K, et al (2015) studied the evaluation and adoption of rapid production by explaining the five consecutive evolutionary steps that should be understood to capitalize on the potential associated with rapid production technology [5].

Swee Leong Sing, et al (2017) studied direct laser sintering or melting of ceramics using CO_2 laser beam, which has the promise to fabricate functional ceramic parts directly without any binders or post sintering steps. The used ceramic materials were silica and zirconia. Ceramics are sintered with solid state sintering methods. The melting was conducted under the category of powder bed fusion manufacturing technologies with low temperature, low density and high-power laser beam [8].

Feng Ma, et al (2018) studied the relationship between main sintering parameters and energy consumption and material cost. Here they discussed three variables, scanning speed, gap distance and layer thickness which are affect the energy consumption and material cost [10].

Danezana. A, et al (2017) in these studies the laser sintering procedure was investigated using commercial porcelain powder with no additions. The powder features, such as particle size distribution and shape, were important factors in this fabrication process [11].

Fina. F, et al (2018) demonstrate the feasibility of SLS to fabricating novel solid dosage forms with accelerated drug release properties, and with a view to create orally disintegrating formulations. Two polymers hydroxypropyl methylcellulose and vinylpyrrolidone-vinyl acetate copolymer were used [12].

Chao Cai, et al (2021) Studied a systematic benchmark and comparison of polyamide 12 (PA12) parts printed by SLS and MJF was conducted on the physicochemical characterization of raw powder materials and their printed specimens. Both designated-supply PA12 powders for each technique were found to have nearly comparable thermal characteristics, phase constitutions, functional groups, and chemical states [22].

RESULTS AND DISCUSSION:

Temperature

In the SLS process, a scanned laser beam totally melts or sinters and solidifies the material locally in a powder bed according to the 3D-CAD model [22]. Temperature affects bulk material thermal properties such as thermal conductivity and heat capacity [23]. High temperatures produce powder agglomeration, which reduces the flowability of the powder. The mechanical integrity, dimensional precision, and surface polish of printed components have all been known to be affected by high processing temperatures. Thus, the properties of laser sintered polymers must be improved, maintained, or restored. Cross-linking of molecular chains also enhances the viscosity of the melt. As a result, the printed components' tensile strength improves at the price of their percentage elongation at break. Thus, high processing temperatures for lengthy periods of time reduce the reusability of polymer materials utilized in SLS. Because SLS occurs at a high temperature, polymers should have a high temperature breakdown point. A sufficiently large sintering window characterizes suitable polymers, preventing quick crystallization of the polymers during processing, which would otherwise induce shrinkage and part-curling. In addition, suitable polymers should have a restricted melting

point area to avoid the need for high laser energy while fusing powder particles [24].

The process temperatures must be kept between the melting and crystallization points of the material. Powder with limited flowability has a detrimental impact on powder spreading and increases the coalescence of powder particles during the SLS process. Low-temperature laser sintering degrades powder at a slower rate than high-temperature laser sintering. Due to reduced viscosity and less coalescence of the powder particles, low temperature SLS improves the recyclability of polymeric materials in the expanse of inferior mechanical and physical qualities of the generated products [24]. Under laser irradiation, powder particles melt quickly, forming a melt pool along the laser scanning tract. The melted polymer cools to room temperature after sintering. The polymer undergoes a phase change from liquid to solid during the cooling process. Thermal contraction of the solid-state polymer is also not uniform. Furthermore, in semicrystalline polymers, sections of molecular chains fold together in an orderly pattern to form a crystalline phase. The volume of the polymer shrinks significantly as a result of the crystallization process. Dimensional accuracy, porosity, surface roughness, microstructure, and mechanical behaviour of SLS printed products are all affected by these behaviours [25].

Increased temperatures near the melting point and long reaction times, as in SLS, provide ideal circumstances for the post-condensation chain extension. The chain mobility in the solid is boosted as a result of the high temperature in the construction chamber, and reactive end groups may encounter and react with another one. The molecular weight of the powder increases as a result of this so-called solid-state post-condensation, resulting in increased viscosity and, in extreme situations, gel forming. The viscosity of the SLS powder, especially when used multiple times, grows to the point that no homogeneous laser melt track can form during the melting phase of the laser sintering process [26].

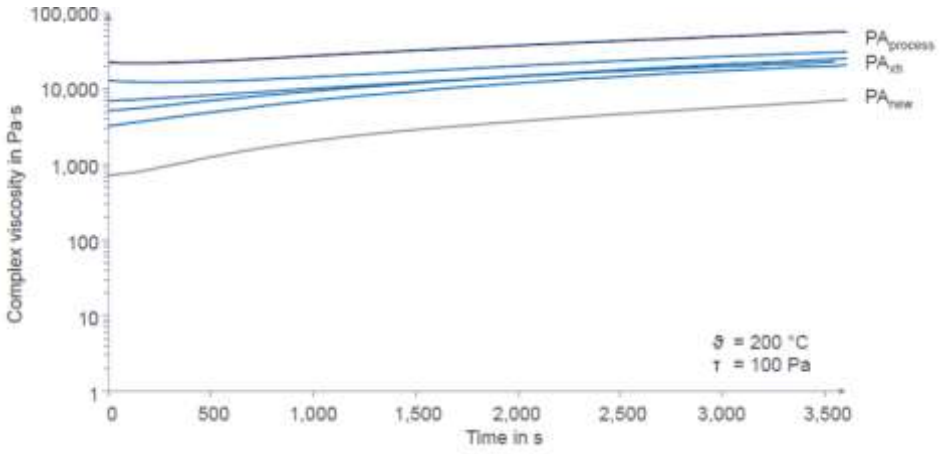

Figure 1: The longer the storage time the higher the viscosity [26].

description & power state

- PA new- virgin powder

- PA xh - Powder that has been stored in the oven for several hours.

- PA process - Powder that has been taken from a real selective laser sintering process.

The viscosity profiles of the powders are shown in the figure 1. The viscosity increases with increasing measuring time in all measurement. The powders can be classified into 3 viscosity categories. The colours black, bright blue and dark blue are used in the diagram. The viscosity of PA new (black) is by far the lowest. The viscosity profiles of the powders following oven storage are depicted by the bright blue. Over time, an increase in viscosity can be seen due to a post- condensation effect caused by heat storage [26].

Scanning speed

For linear dimensions, scanning speed is an important parameter. The porosity and surface defects are primarily caused by increase laser scanning speed. The lower the scanning speed will longer the melting time. The laser energy transmission takes less time for the fast-scanning speed. As a result, the laser energy is insufficient,

resulting in melt spreading failure [27]. Due to low liquid velocity, a long liquid lifetime and resultant elevated thermal stress, a microscopic balling phenomenon and interlayer thermal micro cracks were formed due to combination of consequent high laser energy density and less scanning speed. In contrast, using a fast-scanning speed, resulted in disorderly liquid solidification and considerably large balling due to an elevated instability of the liquid induced by Marangoni convection. Using measurements of microscopic parameters such as, surface topology and structure, as well as mechanical properties such as, thickness and coarseness, the impact of scanning speed was continuously assessed. With the faster scanning speeds, the splashing effect mechanism decrease. This flashing affect is formed by the interaction of a high velocity laser with a rapidly heated power that swelled in volume and drove the powder that swelled in volume and was driven to the cementing layer on the final surface. This was mostly because of the strain of recoil generated by rapid melting or even steaming of the laser power and powder [28].

The higher scanning speed, smaller the molten pool, which reduce the wettability and flow of the molten pool during the SLS process. At the same time, molten pool droplets are easily splashed, and microstructure spheroidization, unfused flaws, and gas holes are common in microstructures [29].

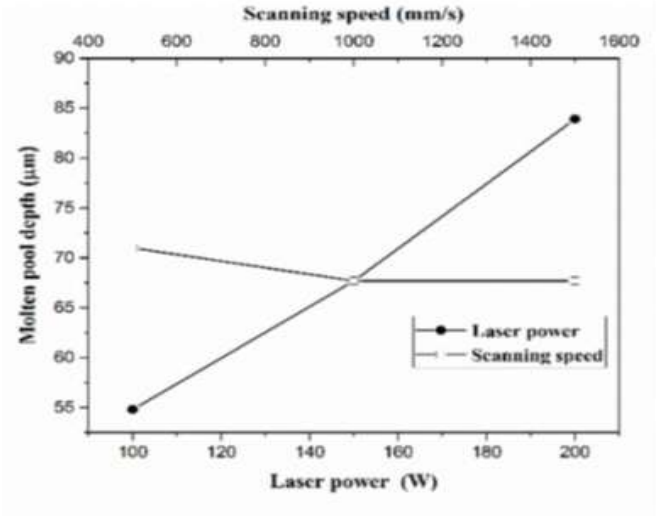

Figure 2: The relationship of molten pool depth with the scanning speed and laser power [30]

Difference scanning speed and laser power with melting pool is shown in figure 1. The scanning speed has less significant effect on them than laser power [30].

The laser energy density increases when the scanning speed is decreased, allowing for more time to melt powder particles and grain growth. Due to the less scanning speed, the powder melts better and spread more consistently in the making process, which makes the final solidified structure broader and tighter the bonding. Thus, the microstructures are free of stomata and defects. The mechanical properties increase as scanning speed decrease, which is consistent with the microstructure. In order to achieve reduced pore defect, a larger melt pool, grater mechanical characteristics and high efficiency, it is preferable to reduce scanning speed [30].

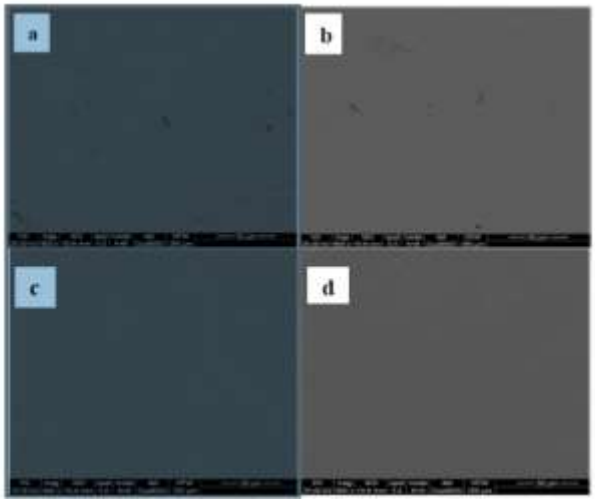

Figure 3: Cross section of products at different scanning speed (a)2000mm/s (b)1800mm/s (c)1400mm/s (d) 1000mm/s [29].

The cross section of 4 samples at various scanning speeds are shown in figure 2. The microstructures of the 4 products are homogeneous, as shown in figure. When the scan speed is 2000mm/s or 1800mm/s, the products have some holes and minor crackers, however when the scanning speed is 1400mm/s or 1000mm/s, the products have no noticeable holes or cracks. It is obvious that as the scanning speed slows, the number of holes in the products lowers. The effect of scanning speed on laser energy is mostly responsible for this. Faster the scanning speed shorter the time of the laser energy transfer [29].

Laser power

The rate at which the laser is able to draw the cross section of the part is referred to as laser power [31]. It's an important metric to determining how much energy powder absorbs during the sintering process. The density of laser energy increases as laser power increases, allowing for longer time to melt powder particles and grain growth. Thus, high laser energy density is beneficial for pore reduction. The mechanical properties increase as the laser power increases, which is consistent with the microstructure. That means the laser power gas a greater impact on mechanical properties. Therefore, it is better to increase laser power in order to produce less pore defect, a larger melt pool and higher mechanical characteristics while maintaining high efficiency [30].

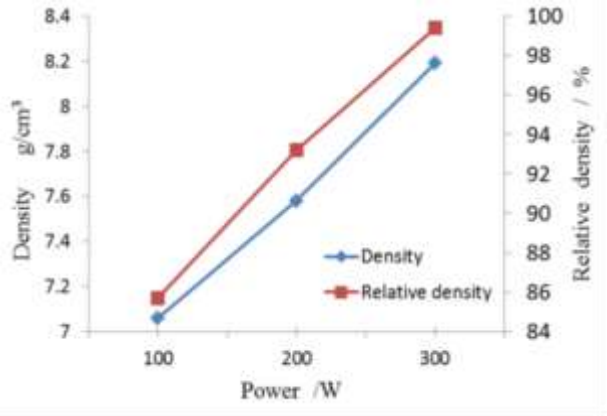

Figure 4: Effect of laser power on relative Density and density of an alloy [29]

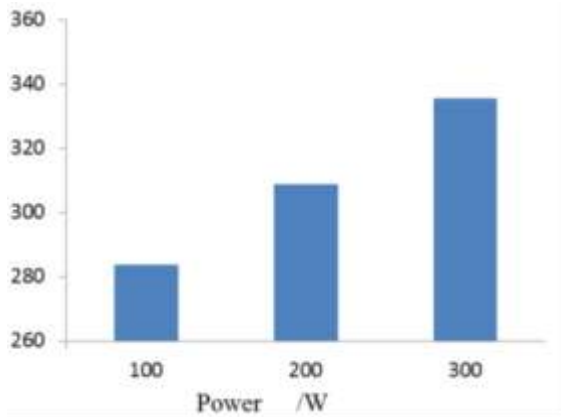

Figure 5: Effect of laser power on hardness of an alloy [29]

The density and the hardness graphs are shown in the figure. The relative density and density of the product increase as increase of power and hardness of the product [29]. As, laser power increases, more heat penetrate the machine bed, increasing the potential for powder particles to become closely packed. Therefore, complex organized pieces with increased density and hardness emerge [32].

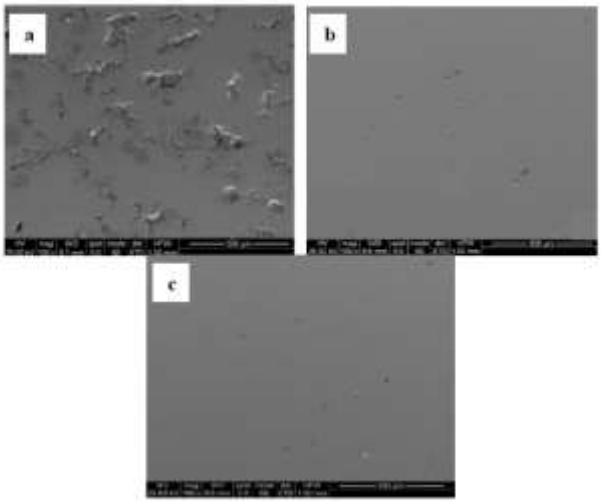

Figure 6: Interior structure of an alloy under variable laser powers (a) 100W, (b) 200W (c) 300W [29]

Figure 6 depicts the interior structure of 3D printing products. Under the condition of 100W laser power, numerous holes can be seen in the product and the holes contain more un-melted spherical powder particles. The porosity of the product drops significantly when the laser power is increased from 200W to 300W, the microstructure is consistent and there are no visible pore, inclusion or un-melted particle. The energy absorption of powder in the sintering process is reflected by laser power. When the laser power is too low, the powder melts incompletely, which resulting in un-fused defects and pore formation in the alloy. As a result, the powder bed absorbs insufficient laser energy and the wettability between the molten pool and the substrate is low, which cause to form spherical particles. When the laser power is too high, the surplus heat can't be transferred in time, resulting in the easy occurrence of over burning [29].

Dimensional errors

Among various three-dimensional printing technologies in additive manufacturing (AM), selective laser sintering (SLS) is found to be better in fabrication.[33] However dimensional errors are a common anomaly which causes horizontal as well as vertical deformations. These errors result from numerous factors such as material property, temperature control and inherent AM technology.[39] Therefore, dimensional accuracy can be defined as the degree of coherency or corollary between the present dimension sample fabricated and the original sample with specific design specifications proposed to be manufactured. A series of steps are performed for formulating a relevant compensational algorithm by which we can minimise these dimensional inaccuracies. [35] First of all, the reference or desired sample to be produced is designed using CAD software in terms of part geometry, roughness and contours of top and bottom surfaces. Afterwards quadratic, cubic or polynomial mathematical equation is formulated and thus regression model is defined. Again, compensation algorithm is deduced using Matlab programming. Eventually, the CAD file of reference sample is re meshed using certain software and the primary compensation algorithm is modified to obtain actually manufactured sample. Now, both the reference and actually produced samples are three dimensionally printed by SLS. Both the samples are finally scanned in the scanner and their percentage differences can be analysed.[37]

In this paper, the process parameters have been pre-defined such as sPro230 was the SLS machine taken, material to be fabricated was Duraform PA, layer thickness of sample to be produced was 0.1 mm, laser power inner side was 10 W and outer side was 4W, laser scan speed was 6mm/sec, build chamber temperature was 171^ C – 174^C, tensile strength was 43 MPa. The three-dimensional model surfaces are composed of many triangular planes. Point based compensation model can be obtained on curling pattern. It is applied to both x and y direction, where corresponding co efficient are substituted into proposed algorithm. [36]

Curvature in x direction Zx $- a_x^2 + b_x + c$

Curvature in y direction Zy $- a_y^2 + b_y + c$

Curvature in z direction $- a_x (x_i - X_l)^2 + a_y (y_i - Y_l)^2$

Here, co efficient a controls degree of curvature of function such that value of 'a' is positive, which implies curvature is upward and value of 'a' is

negative which implies curvature is downward. Similarly larger magnitude of 'a' indicates a sharp curve and smaller magnitude of 'a' indicates a uniform curve. Again coefficients 'b' and 'c controls location of symmetry and height of curvature. Here X_l and Y_l are coordinates of centroid. [36]

Here 4 samples are taken into account. For sample (S1), the front surface is called top and rare surface is called bottom. These are analysed in x axis and y axis. Thus, square of regression coefficient in x axis are named as x1 and x2. Again, square of regression coefficient in y axis are named as y1 and y2. Thus, there are 4 variables for surface S1. Similar is the case for surfaces S2, S3 and S4. The values of the percentage square of linear, quadratic and cubic coefficients (R%) in all specified directions have been recorded in Table 1.

Finally, a frequency distribution graph is plotted with square of regression coefficient (R^2) for linear and quadratic form in Figure 7. Also, a frequency distribution graph is plotted with square of regression coefficient (R^2) for Linear and Cubic form in Figure 8. Again, in Figure 9 and Figure 10, for given surface S1 and S2, all the three linear, quadratic and cubic regressions are plotted in form of cylindrical bar graphs.

Sample	Direction	Surface	Linear	Quadratic	Cubic
S1	x1	Top	90.5	99.4	99.5
	x2	Bottom	37.2	99.5	99.7
	y1	Top	0.8	94.1	94.2
	y2	Bottom	2.1	99.3	99.4
S2	x1	Top	2	94.1	94.5
	x2	Bottom	74.9	99.9	99.9
	y1	Top	1.7	94.7	95.2
	y2	Bottom	48.7	99.5	99.6
S3	x1	Top	90	99.3	99.4
	x2	Bottom	62.1	99.7	99.8
	y1	Top	91.8	99.6	99.6
	y2	Bottom	68	99.8	99.9
S4	x1	Top	0.8	93	93.1
	x2	Bottom	56.3	99.6	99.7
	y1	Top	93.8	99.7	99.7
	y2	Bottom	63.2	99.8	99.9

TABLE 1: The values of the percentage square of linear, quadratic and cubic coefficients (R%) in all specified directions

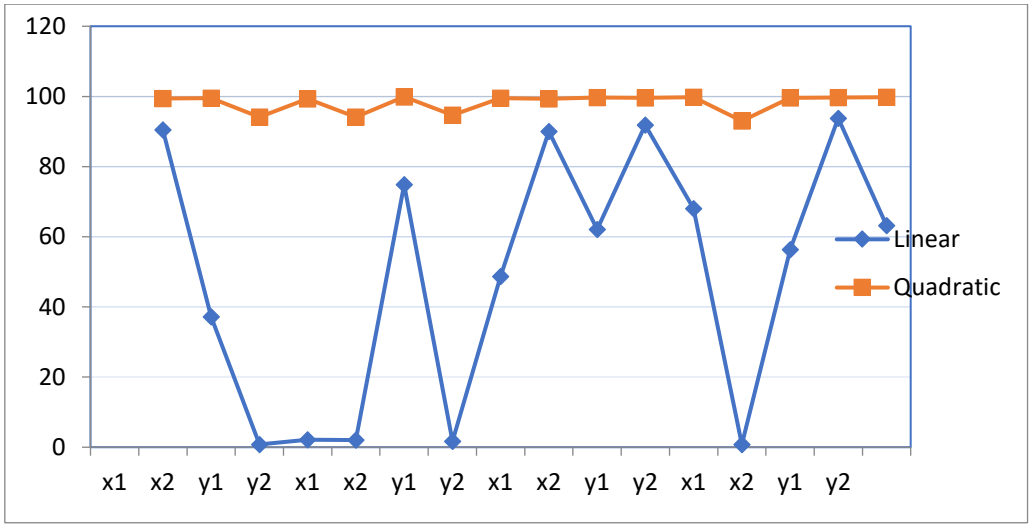

Figure 7: frequency distribution graph with square of regression coefficient (R^2) for linear and quadratic form

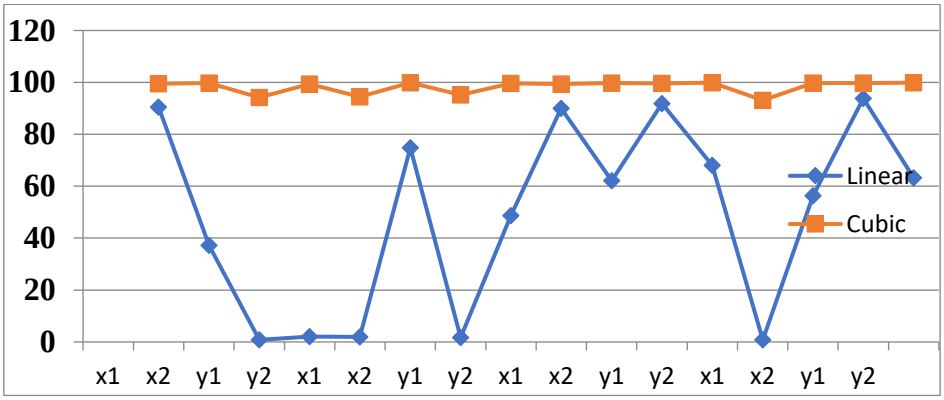

Figure 8: a frequency distribution graph is plotted with square of regression coefficient (R^2) for Linear and Cubic form

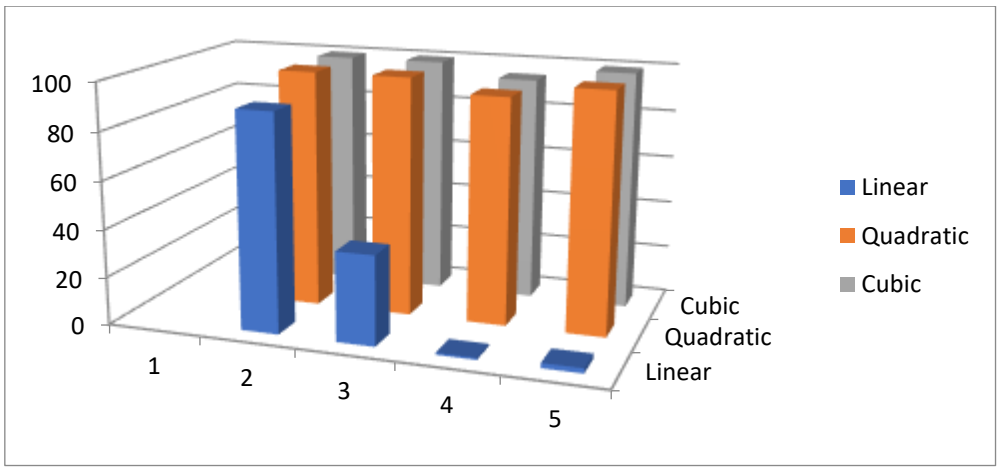

Figure 9: for given surface S1, all the three linear, quadratic and cubic regressions in form of cylindrical bar graphs.

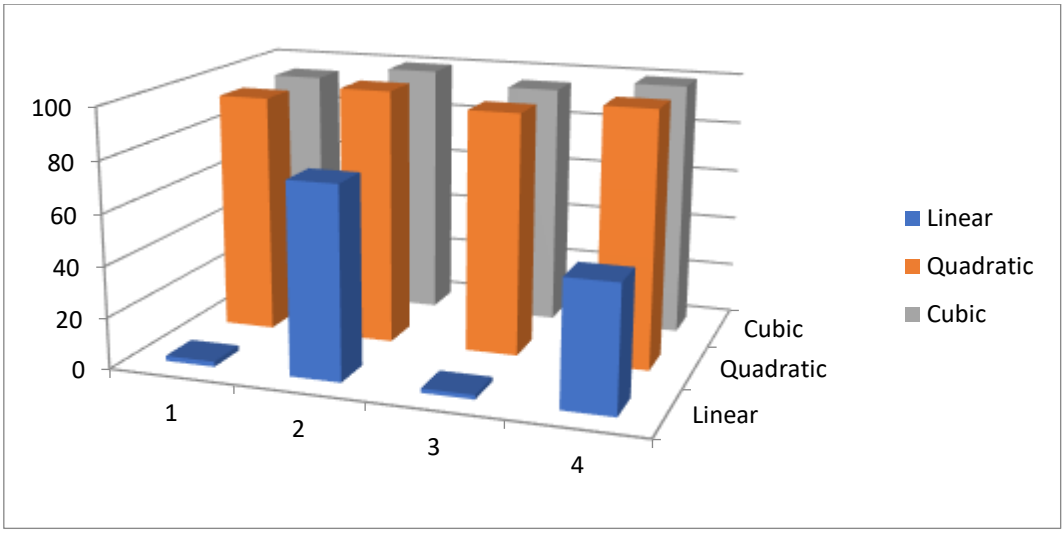

Figure 10: for given surface S2, all the three linear, quadratic and cubic regressions in form of cylindrical bar graphs.

Considering all the 4 given samples for all top and bottom surface in X and Y axis, the percentage square of regression coefficients (R %) is evaluated. Findings can be summed up as-

The linear frequency distribution curve is showing many abrupt values ranging from 0.8-93.8.

The quadratic and cubic curves are showing almost constant values with minimum deviations in the range of 93.0-99.9

Similarly for sample S1 and S2, R% is evaluated for a particular surface e.g. top surface of X axis and the findings can be summed up as-

The linear bar graph values attain from 1.7, 32, 63.2 and 75. There is no consistency in the data.

The quadratic and cubic bar graphs display almost similar values of 95-99, in a well-defined range.

Density and layer thickness

Additive manufacturing (AM) is a kind of process that has evolved from rapid prototyping. Selective laser sintering (SLS) is one of the processes of AM. Laser scanning speed and laser powder are the most effective parameter on density of fabricated parts.[33] An empirical modelling consisting of linear or polynomial function is formulated to study SLS process. Here response surface methodology (RMS) is introduced in which a relationship is described between independent input variable and the response shown by output variables. The input parameters selected are scan speed, current and frequency. Output parameters to be investigated are layer thickness, density and laser power.[34]

In this paper a face cantered central composite design (CCD) was used. There were three levels in coded form (-1, 0, 1) which represents low, medium and high level of a parameter. Current is taken as 8, 9 and 10 A, frequency is set as10, 15 and 20 kHz and scan speed is calibrated as 100, 300 and 500 mm/sec [39]

A statistical modelling was carried to derive relation between the selected parameter and response of the experiment. A quadratic regression model is formulated as follows-

$$Ɒ = \beta_0 + \sum_i^k \beta_i x_i + \sum_i^k \beta_{ii} x_i^2 + \sum_{i<i<j}^k \beta_{ii} x_i x_j + \varepsilon$$

where k is the number of variables, b0 is the constant term, bi represents the coefficients of the linear term, bii represents the coefficients of the quadratic parameters, bij represents the coefficients of the interaction term, xi.j represents the variables i and j and 1 is the residual associated with the experiments. [38]

Basically, under different input parameters ranging from lower, medium to large values, output parameters are being analysed. Also, certain input parameter e.g., scan speed is kept constant and other input parameters like current and frequency are varied from minimum to maximum range and then values are recorded by ANOVA methods for all output parameters such as layer thickness, density and power. The results of same are present in Table 2.[40]

Scan Speed	Current	Frequency	Layer thickness	Density	Power
mm/s	A	kHz	mm	g/cc	W
500	8	5	0.1	3.55	2.56
500	10	5	0.22	3.65	4
300	9	5	0.198	3.6	5.4
500	9	10	0.119	4.1	6.48
500	8	15	0.105	4.5	7.68
300	8	10	0.153	3.8	8.53
300	9	10	0.208	4.4	10.9
300	9	10	0.21	4.41	10.72
300	9	10	0.206	4.409	10.8
300	9	10	0.206	4.42	10.97
300	9	10	0.205	4.41	11
300	9	10	0.204	4.41	10.7
500	10	15	0.23	6.1	12
100	8	5	0.25	3.62	12.8
300	10	10	0.288	5	13.33
300	9	15	0.243	5.75	16.2
100	10	5	0.45	3.9	20
100	9	10	0.35	5.3	32.4
100	8	15	0.3	5.9	38.4
100	10	15	0.49	7	60

TABLE 2: Current and frequency are varied from minimum to maximum range and then values are recorded by ANOVA methods for output parameters layer thickness, density and power

Again, graphs are plotted to investigate the effects of scan speed, frequency of scan and current on the layer thickness as well as density of fabricated parts. Two of the input parameters are varied from increasing to decreasing range, while one of the inputs is kept at a constant value. For example, when scan speed and frequency will be varying, current will be kept constant. Now, the area graphs are analysed independently with respect to layer thickness as well as density of the material. Results are shown in Figure 5, 6, 7 and 8 [40].

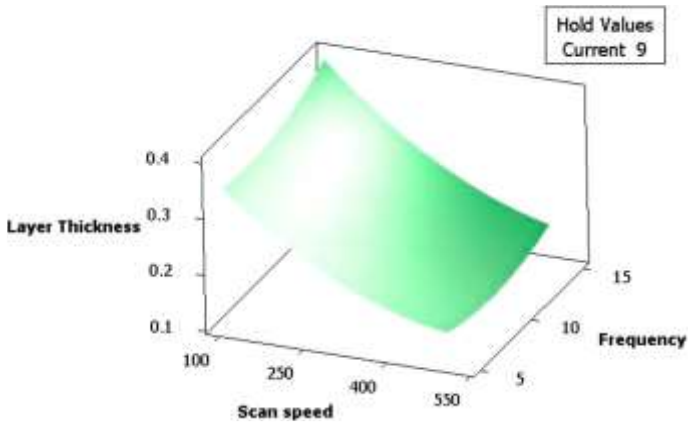

Figure 11: The effects of scan speed and frequency on layer thickness [40].

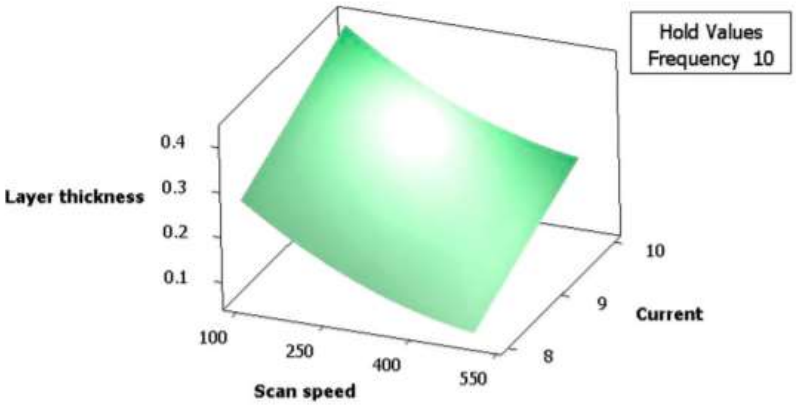

Figure 12: The effects of scan speed and current on layer thickness [40].

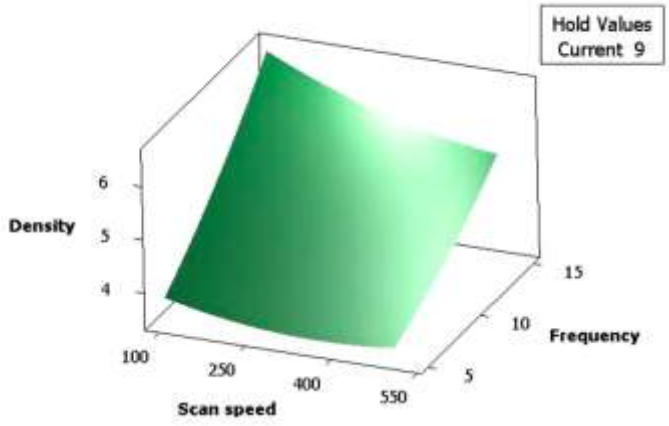

Figure 13: The effects of scan speed and frequency on Density [40].

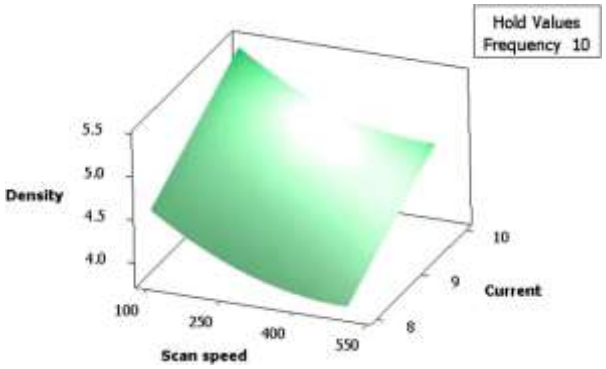

Figure 14: The effects of scan speed and current on density [40].

At constant frequency of 5 kHz, 80% increases in scan speed leads to 70% decreases in layer thickness.

At a constant scan speed of 100 mm/s, 20% increases of current leads to 66% increases of layer thickness.

At a constant frequency of 15 kHz, 80% increases in scan speed leads to 15% decreases in density.

At a constant scan speed of 100 mm/s, 20% increases of current leads to 18% increases in the density.

By careful examination of area graphs, various findings were observed [40]

Thus, it is analysed by increasing laser frequency leads to higher power density in a location. By increasing power density, the penetration of laser in the powder increases and consequently layer thickness increases. It can be concluded that at constant frequency, an increase in scan speed leads to decrease in layer thickness. Similarly scan speed controls the geometry of molten pool. At lower scan speed, materials stay more time molten. These effects lead to lower thickness in higher scan speeds. Again, increase in current leads to more power density and higher layer thickness.[39]

CONCLUSION

This work represents a comprehensive literature review of the effects of variable parameters on selective laser sintering. The discussed parameters were laser power, scanning speed, and temperature. It was concluded that high temperatures cause agglomeration of powder, which leads to a decrease in the flowability of powder and also affects the mechanical integrity, dimensional accuracy, and surface finish of printed components. The lower the scanning speed, the longer the melting time, and the faster the scanning speed, the shorter the time of the laser energy transfer. The higher scanning speed, smaller the molten pool, which reduce the wettability and flow of the molten pool during the SLS process. When the laser power is too low, powder melts are incomplete, resulting in un-fused defects and pores in the alloy; when the laser power is too high, excess heat cannot be transferred in time, resulting in over-burning

REFERENCES

[1] Song J.L., Li Y.T., Deng Q.L., Hu D.J. (2007) Rapid prototyping manufacturing of silica sand patterns based on selective laser sintering, vol 187, p 614-616, 10.1016/j.jmatprotec.2006.11.108 Journal of Materials Processing Technology (Accessed by Nov 2021)
[2] Vo Tuyen., Thanh Nam Nguyen., Khanh Dien Le. (2019) Research on the Design of the Laser Beam in SLS Rapid Prototyping Machine, vol 894, p 140-148, 10.4028/www.scientific.net/AMM.894.140 Applied Mechanics and Materials (Accessed by Nov 2021)
[3] Sercombe. T.B (2011) Laser sintering and rapid prototyping of aluminium, p 702-718, 10.1533/9780857090256.3.702, (Accessed by Nov 2021)
[4] Nitish Kumar., Hemant Kumar., Jagdeep Singh Khurmi., (2016) Experimental Investigation of Process Parameters for Rapid Prototyping Technique (Selective Laser Sintering) to Enhance the Part Quality of Prototype by Taguchi Method, vol 23, p 352-360, 10.1016/j.protcy.2016.03.037 (Accessed by Nov 2021)
[5] Muita K., Westerlund M., Rajala R., (2015) The Evolution of Rapid Production: How to Adopt Novel Manufacturing Technology, vol 48, p 32-37, 10.1016/j.ifacol.2015.06.054. (Accessed by Nov 2021)
[6] Williams J.V., Revington P.J., (2010) Novel use of an aerospace selective laser sintering machine for rapid prototyping of an orbital blowout fracture, p 182-4; 10.1016/j.ijom.2009.12.002. Epub 2010 Jan https://pubmed.ncbi.nlm.nih.gov/20064702/ (Accessed by Dec 2021)
[7] Mona Saffarzadeh., Greg Gillispie., Philip Brown., (2016) Selective leaser sintering (SLS) rapid prototyping technology: a review of medical applications. (Accessed by Dec 2021)
[8] Sing, S.L., Yeong, W.Y., Wiria, F.E., Tay, B.Y., Zhao, Z., Zhao, L., Tian, Z. and Yang, S. (2017) Direct selective laser sintering and melting of ceramics, Vol. 23, p 611-623, 10.1108/RPJ-11-2015-0178/full/html, Rapid Prototyping Journal, (Accessed Dec by 2021)
[9] Fabrizio Fina., Alvaro Goyanes., Simon Gaisford., Abdul W. Basit (2017) Selective Laser Sintering (SLS) 3D printing of medicines, vol 529, p 285-293, 10.1016/j.ijpharm.2017.06.082. (Accessed by Dec 2021)
[10] Feng Ma., Zhang, Hua., Hon, K.K.B., Gong, Qingshang (2018) An optimization approach of selective laser sintering considering energy consumption and material cost, vol 199, 1 0.1016/j.jclepro.2018.07.185, Journal of Cleaner Production (Accessed by Dec 2021)
[11] Danezana. A., Delaizir G., Tessier-Doyen N., Gasgnier G., Gaillard J.M., Duport P, Nait-Ali B, (2017) Selective laser sintering of porcelain, vol 38, p 769-775, 10.1016/j.jeurceramsoc.2017.09.034. (Accessed by Dec 2021)
[12] Fina. F., Madla C.M., Goyanes A., Zhang J., Gaisford S., Basit A.W, (2018) Fabricating 3D printed orally disintegrating printlets using selective laser sintering p 101-107, 10.1016/j.ijpharm.2018.02.015, (Accessed by Dec 2021)
[13] Chao Cai., Wei Shian Tey., Jiayao Chen., Wei Zhu., Xingjian Liu., Tong Liu., Lihua Zhao., Kun Zhou, (2021) Comparative study on 3D printing of polyamide 12 by selective laser sintering and multi jet fusion, vol 288, 10.1016/j.jmatprotec.2020.116882. (Accessed by Dec 2021)
[14] An-Nan Chena., Jia-Min., Liu, Kai., Chen, Jing-Yan., Xiao, Huan., Chen, Peng., Chenhui, Li., Shi, Yusheng (2017) High-performance ceramic parts with complex shape prepared by selective laser sintering: a review, vol 117, p 18, 10.1080/17436753.2017.1379586, Advances in Applied Ceramics (Accessed by Dec2021)
[15] Aoulaiche Mokrane., M'hamed Boutaous., Shihe Xin (2018) Process of selective laser sintering of polymer powders: Modelling, simulation, and validation, vol 346, p 1087-1103, 10.1016/j.crme.2018.08.002. (Accessed by Dec 2021)
[16] Hupfeld. T., Laumer T., Stichel T., Schuffenhauer T., Heberle J., Schmidt M., Barcikowski S., Gokce B, (2018) A new approach to coat PA12 powders with laser-generated nanoparticles for selective laser sintering, vol 74, p 244-248, 10.1016/j.procir.2018.08.103, (Accessed by Dec 2021)
[17] Olakanmi. E. O., Cochrane R.F., Dalgarno K.W, (2015) A review on selective laser sintering/melting (SLS/SLM) of aluminium alloy powders: Processing, microstructure, and properties, vol 74, p 401-477, 10.1016/j.pmatsci.2015.03.002 (Accessed by Dec 2021)
[18] Shangqin Yuan., Fei Shen., Jiaming Bai., Chee Kai Chua., Jun Wei., Kun Zhou., (2018) 3D soft auxetic lattice structures fabricated by selective laser sintering: TPU powder evaluation and process optimization, vol 120, p 317-327, 10.1016/j.matdes.2017.01.098, (Accessed by Dec 2021)
[19] Zhang. Z., Yao X.X., Ge P, (2019) Phase-field-model-based analysis of the effects of powder particle on porosities and densities in selective laser sintering additive manufacturing, vol 166, 10.1016/j.ijmecsci.2019.105230, (Accessed by Dec 2021)
[20] Fei Shen., Yuan, Shangqin., Chua, Kai., Zhou, Kun (2017) Development of process efficiency maps for selective laser sintering of polymeric composite powders: Modelling and experimental testing, vol 254, 10.1016/j.jmatprotec.2017.11.027, Journal of Materials Processing Technology (Accessed by Dec 2021)
[21] Paul. K, (2021). Rapid prototyping, https://en.wikipedia.org/wiki/Rapid_prototyping (Accessed by Jan 2022)
[22] Chivel Yu., Smurov I. (2010) On-line temperature monitoring in selective laser sintering/melting, Physics Procedia, Vol 5, Part B, P Pages 515-521, ISSN 1875-3892,

https://doi.org/10.1016/j.phpro.2010.08.079.(Accessed by Jan 2022)
[23] Kolossov S., Boillat E., Glardon R., Fischer P., Locher M. (2004) 3D FE simulation for temperature evolution in the selective laser sintering process, International Journal of Machine Tools and Manufacture, Vol 44, Issues 2–3, P 117-123, ISSN 0890-6955, https://doi.org/10.1016/j.ijmachtools.2003.10.019. (Accessed by Jan 2022)
[24] Fredrick M. Mwania., Maina Maringa., Kobus van der Walt. (2020) A Review of Methods Used to Reduce the Effects of High Temperature Associated with Polyamide 12 and Polypropylene Laser Sintering, vol 2020, Article ID 9497158, 11 pages. https://doi.org/10.1155/2020/9497158. (Accessed by Jan 2022)
[25] Shen, F., Zhu, W., Zhou, K. (2021) Modelling the temperature, crystallization, and residual stress for selective laser sintering of polymeric powder. Acta Mech 232, 3635–3653. https://doi.org/10.1007/s00707-021-03020-6. (Accessed by Jan 2022)
[26] Benz J., Bonten C. (2019) Temperature induced ageing of PA12 powder during selective laser sintering process. AIP Conference Proceedings 2055, 140001; (Accessed by Jan 2022)
[27] Yuan W., Chen H., Cheng T. (2020) Effects of laser scanning speeds on different states of the molten pool during selective laser melting: Simulation and experiment, Materials & Design, Vol 189, https://doi.org/10.1016/j.matdes.2020.108542. (Accessed by Jan 2022)
[28] Sadali M., Hassan M., Ahmad F., Yahaya,H., & Rasid, Z. (2020). Influence of selective laser melting scanning speed parameter on the surface morphology, surface roughness, and micropores for manufactured Ti6Al4V parts. Journal of Materials Research, 35(15), 2025-2035. doi:10.1557/jmr.2020.84 (Accessed by Jan 2022
[29] Jianguo Chen., Xuanbo Wang., Yingcai Pan (2019) Influence of laser power and scan speed on the microstructure and properties of GH4169 alloy prepared by selective laser melting, IOP Conf. Ser.: Mater. Sci. Eng. 688 033064, doi:10.1088/1757-899X/688/3/033064, (Accessed by Jan 2022)
[30] Kang J W., Yi J H., Wang T J., Wang X., Feng T., Feng Y L., Wu P Y. (2019) Effect of laser power and scanning speed on the microstructure and mechanical properties of SLM fabricated Inconel 718 specimens, Material Science & Engineering International Journal Vol 3, 10.15406/mseij.2019.03.00094, (Accessed by Jan 2022)
[31] Marissa Castoro, (2013) Impact of Laser Power and Build Orientation on the Mechanical Properties of Selectively Laser Sintered Parts. (Accessed by Jan 2022)
[32] Singh, S., Sachdeva, A. & Sharma, V.S. Optimization of selective laser sintering process parameters to achieve the maximum density and hardness in polyamide parts. Prog Addit Manuf 2, 19–30 https://doi.org/10.1007/s40964-017-0020-4, (Accessed by Jan 2022)
[33] C.Y. Yap, C. K. Chua, Z. L. Dong, Z. H. Liu, D. Q. Zhang, L.E. Loh, S. L. Sing (2015); "Review of selective laser melting: Materials and applications.", Page 3, http://dx.doi.org/10.1063/1.4935926
[34] Snehashis Pal, Vanja Kokal, Nenad Gubeljak, Miodra Hadzistevic, Radovan Hudak, Igor Drstvensek (2019); "Dimensional errors in selective laser melting products related to different orientations and processing parameters.", Volume 53, Page 2, https://doi.org/10.17222/mit.2018.156
[35] Cristoph Hartmann, Philipp Lechner, Benjamin Himmel, Yannick Krieger, Tim C Lueth, Wolfram Volk (2019); "Compensation for Geometrical Deviations in Additive Manufacturing.", Page 4-5, https://doi.org/10.3390/technologies7040083
[36] Sangho Ha, Kasin Ransikarbum, Hweeyoung Han, Daeil Kwon, Hyeonnam Kim, Namhun Kim (2018); "A dimensional compensation algorithm for vertical bending deformation of 3D printed parts in selective laser sintering", Page 5-6, https://doi.org/10.1108/RPJ-12-2016-0202.
[37] Vishal Sharma, Ramesh Chand, Vishal S Sharma, Anish Sachdeva, Shranjit Singh (2021); "Investigating shrinkage: CAD, Thermal and Volumetric for Selective Laser Sintering of Polyamide parts", Volume 96, Page 5, https://doi.org/10.1007/s40516-020-00136-w
[38] Shranjit Singh, Vishal S.Sharma ,Anish Sachdeva (2018); 'Application of response Surface methodology to analyze the effect of selective Laser Sintering parameters on dimensional accuracy", Page 3, https://doi.org/10.1007/s40964-018-0049-z
[39] Sangho Ha, Eunju Park, Namhun Kim (2020); "Analysis of Shape Deformation from Densification of Additive Manufacturing Parts in Selective Laser Sintering.", Page 6-7, https://doi.org/10.1007/s12541-020-00359-z
[40] S.A.Fatemi, J.Zamani Ashany, A.Jalali Aghchai, A.Abolghasemi (2017); "Experimental Investigation of process parameters on layer thickness and density in direct metal Laser Sintering process: a response surface methodology", Page 3-5, https://doi.org/10.1080/17452759.2017.1293274.
[41] Ankit Kumar Mishra et al. (2021); Review of Advanced Joining Technique for Aluminium Alloys and Its Properties; International Journal of Science, Engineering and Technology 9(4).